2014

Influence of isothermal treatment on MnS and hot ductility in low carbon, low Mn steels

Kristin R. Carpenter
BlueScope Steel, kristinc@uow.edu.au

Chris Killmore
BlueScope Steel

Rian J. Dippenaar
University of Wollongong, rian@uow.edu.au

Publication Details

Carpenter, K. R., Killmore, C. R. & Dippenaar, R. (2014). Influence of isothermal treatment on MnS and hot ductility in low carbon, low Mn steels. Metallurgical and Materials Transactions B: Process Metallurgy and Materials Processing Science, 45 (2), 372-380.

Influence of isothermal treatment on MnS and hot ductility in low carbon, low Mn steels

Abstract
Hot ductility tests were used to determine the hot-cracking susceptibility of two low-carbon, low Mn/S ratio steels and compared with a higher-carbon plain C-Mn steel and a low C, high Mn/S ratio steel. Specimens were solution treated at 1623 K (1350 °C) or in situ melted before cooling at 100 K/min to various testing temperatures and strained at 7.5 x 10-4 s -1, using a Gleeble 3500 Thermomechanical Simulator. The low C, low Mn/S steels showed embrittlement from 1073 K to 1323 K (800 °C to 1050 °C) because of precipitation of MnS at the austenite grain boundaries combined with large grain size. Isothermal holding for 10 minutes at 1273 K (1000 °C) coarsened the MnS leading to significant improvement in hot ductility. The highercarbon plain C-Mn steel only displayed a narrow trough less than the Ae3 temperature because of intergranular failure occurring along thin films of ferrite at prior austenite boundaries. The low C, high Mn/S steel had improved ductility for solution treatment conditions over that of in situ melt conditions because of the grain-refining influence of Ti. The higher Mn/S ratio steel yielded significantly better ductility than the low Mn/S ratio steels. The low hot ductility of the two low Mn/S grades was in disagreement with commercial findings where no cracking susceptibility has been reported. This discrepancy was due to the oversimplification of the thermal history of the hot ductility testing in comparison with commercial production leading to a marked difference in precipitation behavior, whereas laboratory conditions promoted fine sulfide precipitation along the austenite grain boundaries and hence, low ductility.

Disciplines
Engineering | Science and Technology Studies

Publication Details
Carpenter, K. R., Killmore, C. R. & Dippenaar, R. (2014). Influence of isothermal treatment on MnS and hot ductility in low carbon, low Mn steels. Metallurgical and Materials Transactions B: Process Metallurgy and Materials Processing Science, 45 (2), 372-380.

Influence of Isothermal Treatment on MnS and Hot Ductility in Low Carbon, Low Mn Steels

KRISTIN R. CARPENTER, CHRIS R. KILLMORE, and RIAN DIPPENAAR

Hot ductility tests were used to determine the hot-cracking susceptibility of two low-carbon, low Mn/S ratio steels and compared with a higher-carbon plain C-Mn steel and a low C, high Mn/S ratio steel. Specimens were solution treated at 1623 K (1350 °C) or *in situ* melted before cooling at 100 K/min to various testing temperatures and strained at 7.5×10^{-4} s^{-1}, using a Gleeble 3500 Thermomechanical Simulator. The low C, low Mn/S steels showed embrittlement from 1073 K to 1323 K (800 °C to 1050 °C) because of precipitation of MnS at the austenite grain boundaries combined with large grain size. Isothermal holding for 10 minutes at 1273 K (1000 °C) coarsened the MnS leading to significant improvement in hot ductility. The higher-carbon plain C-Mn steel only displayed a narrow trough less than the Ae_3 temperature because of intergranular failure occurring along thin films of ferrite at prior austenite boundaries. The low C, high Mn/S steel had improved ductility for solution treatment conditions over that of *in situ* melt conditions because of the grain-refining influence of Ti. The higher Mn/S ratio steel yielded significantly better ductility than the low Mn/S ratio steels. The low hot ductility of the two low Mn/S grades was in disagreement with commercial findings where no cracking susceptibility has been reported. This discrepancy was due to the oversimplification of the thermal history of the hot ductility testing in comparison with commercial production leading to a marked difference in precipitation behavior, whereas laboratory conditions promoted fine sulfide precipitation along the austenite grain boundaries and hence, low ductility.

DOI: 10.1007/s11663-013-9851-7

I. INTRODUCTION

TRADITIONALLY, the addition of Mn to steels provides solid solution strengthening, ferrite grain refinement (hardenability agent) and prevents hot shortness by the formation of MnS.[1] In hot ductility studies, there has been much emphasis on the effects of S and the formation of MnS, but less attention has been given to steels with low Mn levels. Cowley and Mintz[2] suggest that lower Mn levels would reduce the depth of the ductility trough by limiting the precipitation of MnS within grain-boundary ferrite bands, which facilitate void formation. However, Mintz and Mohamed[3] also argue that lower Mn levels can reduce hot ductility because of the decrease in the grain-refinement ability of the steel.

For as-cast material, a reduction in ductility is often attributed to the segregation of S to austenite grain boundaries leading to the precipitation of sulfide particles at the boundaries. These sulfide particles enhance intergranular failure in austenite by encouraging void formation during grain boundary sliding.[4–8] This mechanism was found to occur in low carbon steels with low Mn/S ratios, where precipitation of MnS at the austenite grain boundaries during cooling to the tensile test temperature caused embrittlement.[9–12] It has also been put forward that S decreases the binding energy between austenite grain boundaries and the matrix, thus promoting intergranular failure.[9] Sulfide inclusions have been shown to be instrumental in affecting hot ductility, but the exact embrittlement mechanism is not fully understood.

In order to design meaningful laboratory hot tensile tests, it is important to simulate slab-straightening conditions during continuous slab casting as closely as possible. Unfortunately, much of the information in the literature seems to suggest that the effect of S content on hot ductility depends largely on test conditions. Such a conclusion is clearly untenable. For example, because S in steel forms precipitates on cooling, such as MnS, test samples that are reheated to solution treatment temperatures, typically between 1523 K and 1623 K (1250 °C and 1350 °C), the degree of dissolution of sulfides determines the amount of sulfur that goes into solution and is subsequently available for re-precipitation as fine sulfides. Accordingly, it is the amount of S that redissolves, not the total S content, which is important for controlling the ductility.[4–8,13,14] Consequently, *in situ* melting, "as-cast conditions" are necessary to incorporate the *total* S content and thus avoid misleading results about the influence of S on hot ductility.[4, 5,7,8,13,14] Banks[14] found that low Mn and

KRISTIN R. CARPENTER, Development Metallurgist, Hot Rolled Product Development and CHRIS R. KILLMORE, Product Design Manager, Hot Rolled Product Development, are with BlueScope Steel, Port Kembla Steel Works, Five Islands Rd, Port Kembla, NSW 2505, Australia. Contact e-mail: kristin.carpenter@bluescopesteel.com RIAN DIPPENAAR, Head of Postgraduate Studies, Higher Degree Research (HDR) Student Coordinator, is with the Faculty of Engineering, School of Mechanical Materials & Mechatronics, University of Wollongong, Northfields Av., Wollongong, NSW 2522, Australia.

Manuscript submitted January 13, 2013.
Article published online April 23, 2013.

high S steels, in particular, required *in situ* solidification test conditions, and hot ductility tests were improved further by incorporating thermal oscillations to better simulate the continuous casting process.

It has been demonstrated that simulating the complex cooling patterns experienced during continuous slab casting affects hot ductility results.[4,10,15–18] For example, Mintz[4,15] and Suzuki[10] both investigated the influence of introducing thermal cycling during cooling to the test temperature, to simulate the thermal oscillation experience by a continuously cast strand from alternating between rolls and water sprays, and both found that ductility was worsened because of increased Nb precipitation. Research by El-Wazri[16,17] and also by Akhlaghi[18] simulated a thermal history where specimens were melted, cooled at ~10 °C/s to a minimum temperature ranging from 973 K to 1173 K (700 °C to 900 °C), reheated to temperatures ranging from 1373 K to 1473 K (1100 °C to 1200 °C), then slowly cooled to the unbending temperature ranging from ~1273 K to 1453 K (~1000 °C to 1180 °C), but no cyclic thermal oscillations were introduced to simulate the thermal pattern because of water spray cooling. The hot ductility values of specimens subjected to these thermal simulations were almost always lower than those predicted by isothermal tests. Despite the known influence of a complex cooling history, much of the hot ductility research has been conducted using a simplified procedure consisting of a heat treatment (solution treatment or *in situ* melting) followed by direct cooling at a fixed rate to the test temperature. While this method usually provides a good indication of the factors affecting the hot ductility trough, results must be validated against commercial experience to avoid erroneous conclusions on the susceptibility of the steels to transverse cracking.

In this research, such simplified simulations for hot ductility testing on low C, low Mn steels were found to greatly misrepresent the grades' propensity for developing transverse cracking, in comparison with plant experience. This discrepancy between hot ductility testing and plant experience, the effect of Mn/S ratio on hot ductility, and the possible embrittlement mechanisms because of S, will be discussed.

II. EXPERIMENTAL

A Gleeble 3500 thermomechanical simulator (Dynamic Systems Inc., Poestenkill, NY) was used to conduct hot tensile testing of the steels listed in Table I. The steels were produced by BOS steelmaking practice and continuously slab cast into 230-mm-thick slabs. The low C, low Mn steels, C1 and C2, had Mn/S ratios of 19.1 and 26.4, respectively. Steel C2 also contained Nb and Ti microalloying elements. A plain C-Mn steel, C3, with a higher carbon content and moderate Mn/S ratio was included for comparison with the low carbon grades. Steel C4 is a conventional HSLA steel with high Mn/S ratio and microalloyed with Nb and Ti.

Samples were either melted *in situ* or solution treated at 1623 K (1350 °C) and cooled at 100 K/min to the test temperature. Samples were held for 1 minute at the test temperature and then strained to failure at a rate of approximately 7.5×10^{-4} s^{-1}, followed by a water quench. The thermomechanical cycle is schematically illustrated in Figure 1. In addition to the above cycles, several samples were subjected to the same cycle except those held isothermally at 1273 K (1000 °C) for 10 minutes before straining. The above time and temperature represent the approximate time taken for a strand to reach the unbending segment for typical continuous casting conditions at BlueScope Steel.

In order to compensate for shrinkage during solidification, a compressive deformation of about 7 pct was applied, while the samples were being cooled at 6 K/s from the melting temperature down to 1643 K (1370 °C). Quartz tubes with a diametrical clearance of 0.2 mm were used to contain the molten zone.

Metallographic examinations were carried out on longitudinal sections taken close to the point of fracture. Fracture surfaces were examined with a Leica Stereoscan 440 (Leica Microsystems Pty Ltd, Wetzlar, Germany) scanning electron microscope (SEM), located at the University of Wollongong. Transmission Electron Microscopy (TEM) was performed at 200 kV on a Joel Scanning Transmission Electron Microscope (Joel, Tokyo, Japan). Electron Probe Micro Analyses, EPMA, was conducted using a Cameca SX-50 (Cameca SAS, Gennevilliers Cedex, France), at BlueScope Steel, Port Kembla, on selected specimens. EPMA Probe settings, featuring high probe currents, are listed in Table II.

III. RESULTS

A. *Hot Ductility*

The hot ductility shown as percentage of reduction of area (Pct RA) as a function of test temperature is shown in Figure 2 for the solution treatment tests. The Ae_3 temperature, included in Figures 2 and 3, was calculated using Andrew's formulae.[19] As seen in Figure 2, steel C3 showed a narrow trough starting at the Ae_3, steel C4 had good ductility at all temperatures, and steels C1 and C2 displayed low ductility at all test temperatures. In most cases, ductility improved at 1023 K (750 °C).

For specimens that were melted *in situ*, much lower ductility values were recorded as shown in Figure 3. All specimens showed low to very low ductility over a wide temperature range, except for C3, which had a deep, narrow trough, similar to that observed for solution treatment conditions. In steel C4, ductility only began to improve at 1273 K (1000 °C), while for steel C2, ductility did not improve significantly until 1323 K (1050 °C). At lower temperatures, ductility began improving at 1023 K (750 °C) for all steel grades, except C4.

B. *Optical Metallography*

Figure 4(a) shows an example of thin films of ferrite forming at austenite grain boundaries, for Steel C3 tested at 1073 K (800 °C) (below the Ae_3 Temperature).

Table I. Chemical Compositions of Steels Used in Hot Ductility Testing (Weight Percentage)

Steel	Type	C	Mn	S	Mn/S	Al (tot)	N	Nb	Ti
C1	1006	0.055	0.21	0.011	19.1	0.032	0.0045	—	—
C2	1008 + Nb + Ti	0.075	0.29	0.011	26.4	0.028	0.0031	0.017	0.01
C3	1016	0.165	0.63	0.012	52.5	0.031	0.0021	—	—
C4	HSLA	0.08	1.39	0.001	1390	0.021	0.0046	0.044	0.018

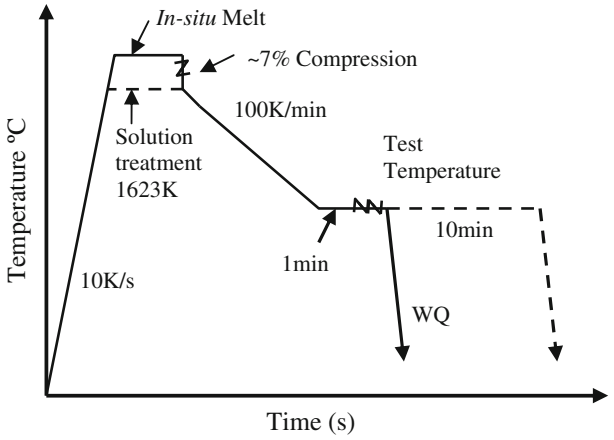

Fig. 1—Schematically illustrated thermomechanical cycle for Gleeble test schedule, including 10-min isothermal hold test.

Table II. EPMA Probe Settings for Mapping of Steel C1

Figure No.	Size (μm)	Current (na)	kV	Pixel (μm)	Dwell (ms)
6	100	100	20	0.38	100
7	100	300	20	0.38	100
8	512	1000	20	2.0	40
9	500	1000	20	2.0	40
10	100	1000	20	0.38	100

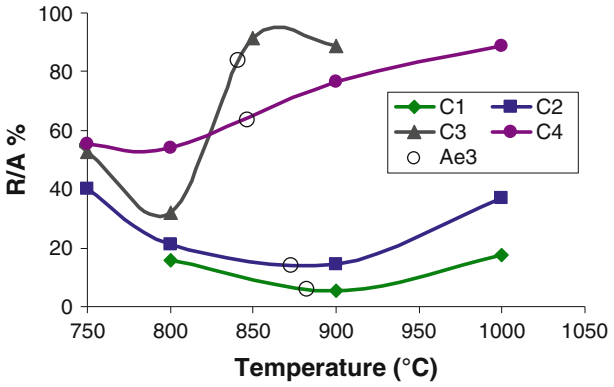

Fig. 2—Hot ductility as a function of test temperature for solution treatment tests, where the Ae_3 temperature calculated from the composition is included.

Figure 4(b) shows intergranular cracking in single-phase austenite in steel C2, which was solution treated and tested at 1173 K (900 °C).

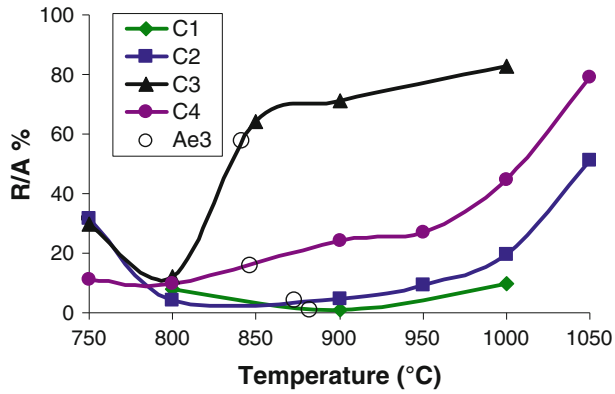

Fig. 3—Hot ductility as a function of test temperature for *in situ* melt tests, where the Ae_3 temperature calculated from the composition is included.

C. *Scanning Electron Microscopy*

The fracture surface of a specimen of Steel 3, which was solution treated and tested at 1073 K (800 °C), is shown in Figure 5(a), which reveals microvoid coalescence, as evidenced by the dimpled intragranular fracture surface. The fracture surfaces of Steels C1 and C2, when tested in the single-phase austenite field, exhibited coarse grain structures and intergranular failure exhibiting smooth, featureless fracture surfaces, Figures 5(b) through (d).

D. *Electron Probe Micro Analysis*

EPMA mapping for Al, Mn, and S was carried out on the C1 grade, and the results are shown in Figures 6 and 7 for tests without isothermal holding, and Figures 8 through 10 for tests with isothermal holding, in both the solution treatment and *in situ* melting conditions.

IV. DISCUSSION

A. *Solution Treatment Conditions*

The relatively high values of hot ductility at 1023 K (750 °C) for specimens that were solution treated are attributed to the increased volume fraction of ferrite that forms at this temperature relative to higher testing temperatures. Steel C4 showed significantly better ductility compared with steels C1 and C2, which was attributed to finer austenite grain size (~200 μm compared with ~500 μm) and the lower sulfur content, both of which strongly favor improved ductility.[3,4,6–8] The finer grain size observed was due to the high

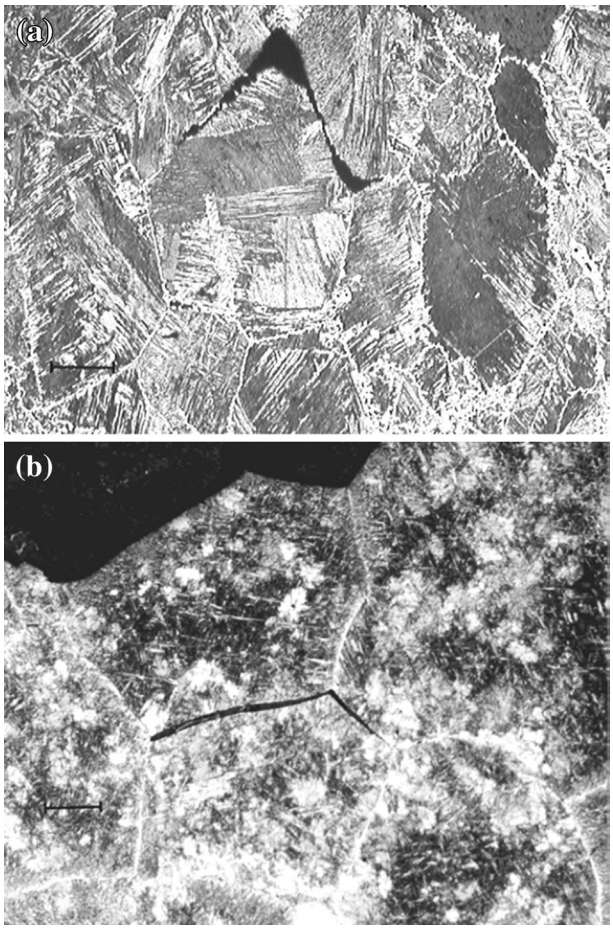

Fig. 4—(*a*) Steel C3: Optical micrograph reveals cracking, ostensibly within ferrite that formed on prior austenite grain boundaries. The specimen was solution treated and tested at 1073 K (800 °C). (*b*) Steel C1 displays severe cracking along prior austenite grain boundaries. The specimen was solution treated and tested at 1173 K (900 °C). (Micron bar scale: 380 μm).

microalloying content restricting grain growth at the solution treatment temperature.

Coarse grains are well known to generate low ductility. In general, hot ductility improves with decreasing grain size as finer grains restrict the propagation of small cracks formed by grain boundary sliding at triple points; reduces the crack aspect ratio, which controls the stress concentration at the crack tip and thereby discourages crack propagation; increases the specific grain boundary area for a given volume fraction of precipitate, resulting in a decrease in the precipitation density on the grain boundary and increase in the number of grain boundary nucleation sites, thereby reducing the critical strain for dynamic recrystallization, which can improve the ductility *via* grain boundary migration.[4,20]

Steel C3 exhibited a narrow ductility trough, between 1023 K (750 °C) and the Ae_3 temperature. Such behavior is conventionally explained because of transformation-controlled intergranular failure, where failure occurs within the thin films of ferrite that form at the prior austenite grain boundaries.[2–4,13] Strain is concentrated at the softer ferrite films, typically leading to failure *via* voiding around particles or inclusions, such as MnS, present at the austenite grain boundaries. Microstructural observations indicate that transformation-controlled intergranular failure has occurred. In Figure 4(a), microstructural observations of the fracture region taken in the longitudinal direction revealed microvoid formation and cracking at thin films of grain boundary ferrite. The fracture surface, Figure 5(a), showed that the fracture mode was intergranular and the shallow dimples appeared on the fracture facets, suggestive of ductile microvoid coalescence.[3,4,13,21–23]

Steels C1 and C2 had very low ductility extending well into the single-phase austenite temperature region. Low ductility in the single-phase austenite temperature region is almost always due to intergranular failure at the austenite grain boundaries. It is generally accepted that cracks are initiated at austenite grain boundaries by the grain boundary sliding mechanism.[3,4,13,22,23]

Severe cracking at austenite grain boundaries were observed by Optical Metallography in Steels C1 and C2, and a typical example of such cracking is shown in Figure 4(b) for Steel C1, tested at 1173 K (900 °C). Figures 5(b) and (c) showed SEM images that revealed smooth, featureless intergranular fracture surfaces indicative of intergranular failure *via* grain boundary sliding in austenite. Grain boundary sliding is promoted by slow strain rates, large grain size, and fine precipitation.[3,4,7,13] The large grain size, as measured optically, was also readily observable in the SEM images and contributed to the low hot ductility. Coarse austenite grains can be detrimental to ductility because cracks due to grain boundary sliding can readily propagate along grain boundaries as there are few triple points to arrest crack propagation. Precipitation enhances crack formation *via* grain boundary sliding by providing crack initiation sites. The role of S on the failure mechanism will be discussed at a later stage.

B. *In Situ Melt Conditions*

The hot ductility curves for the *in situ* melt tests are shown in Figure 3. When melted *in situ*, Steel C3 displayed a slightly deeper ductility trough than when it was solution treated. The larger austenite grain size resulting from *in situ* melting seems to account for this observation.

Steel C4 showed a marked difference in behavior when it was melted and resolidified before testing: a deep, wide trough was observed. The importance of using *in situ* melting conditions for Ti-bearing steels was illustrated by steel C4. The grain-refinement ability of this steel was lost when microalloying particles were dissolved during melting and a significantly larger grain size (up to ~1 mm) was obtained during subsequent re-solidification and cooling. This large grain size contributed significantly to the lower ductility of Steel C4 in the *in situ* treated condition. Carbon extraction replicas were prepared from *in situ* melted specimens tested at 1273 K (1000 °C). Nb-Ti particles less than 10 nm were identified and were often present in small clusters. The enhancement of grain-boundary sliding due to fine, microalloying precipitation is a well-known phenomenon.

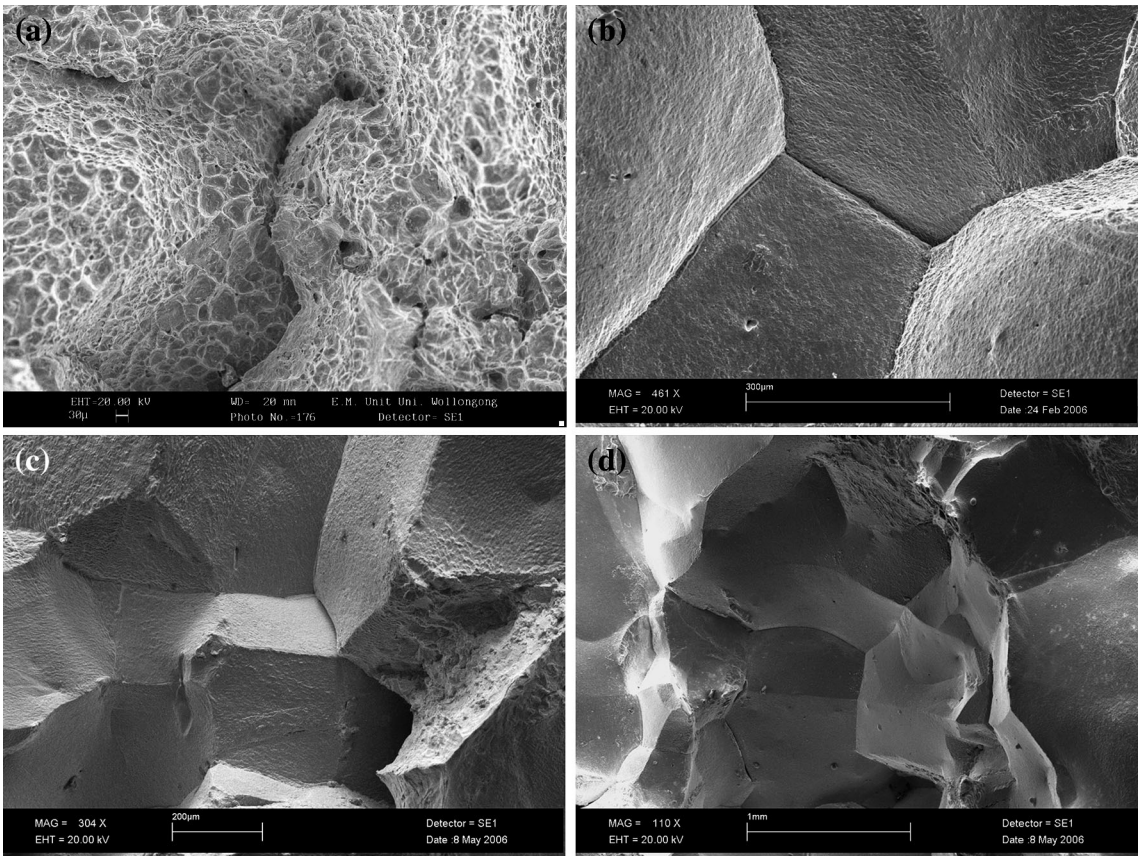

Fig. 5—SEM images of the fracture surface of (*a*) Steel C3, solution treated and tested at 1073 K (800 °C), (*b*) Steel C2, solution treated and tested at 1173 K (900 °C), (*c*) Steel C1, solution treated and tested at 1273 K (1000 °C) and (*d*) Steel C1, melted *in-situ* and tested at 1273 K (1000 °C).

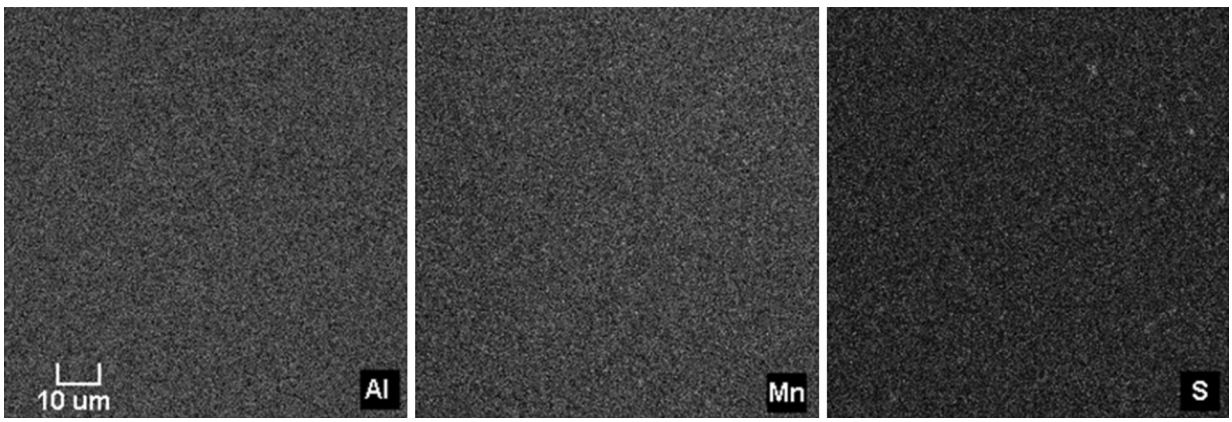

Fig. 6—EPMA image: C1 solution treatment at 1623 K (1350 °C), held for 1 min at 1273 K (1000 °C), and then quenched.

Steels C1 and C2 showed very low ductility at all test temperatures in both the solution treated and *in situ* melted conditions. From Figures 5(c) and 5(d) it can be observed that both test conditions yielded featureless, intergranular fracture surfaces, and a coarse prior austenite grain size, typical of failure *via* grain boundary sliding.[3,13,23] Coarse grains are well known to generate low ductility as previously discussed.

C. *Isothermal Holding Tests*

The low ductility of steels C1 and C2 was a concern because commercial experience has found that there are no ductility issues for these steels during continuous casting. Several solution treatment and *in situ* melt tests were conducted for steel C1 with an isothermal hold at 1273 K (1000 °C) for 10 minutes, before straining.

The subsequent tensile test results showed dramatic improvements in ductility; 67.6 and 60.7 pct for solution treated and *in situ* melt test conditions, respectively. In agreement with earlier findings by Gao and Sorimachi,[24] the significant recovery of ductility was attributed to fine grain boundary MnS particles coarsening to the point where they no longer influence ductility. EPMA was carried out on samples subjected to the isothermal hold schedule, but quenched before deformation, to investigate the behavior of Mn and S.

D. *EPMA Analyses*

Owing to similarities in the Mn and S content of Steels C1 and C2, EPMA mapping for Al, Mn, and S was conducted only for C1, and the results are shown in Figures 6 through 10. EPMA tests on samples without any isothermal holding, Figures 6 and 7, reveal very little evidence of MnS inclusions, within the limitations of EPMA (<100 nm). However, for tests with the isothermal hold, Figures 8 through 10, grain-boundary networks of coarsened MnS particles were evident, leading to Mn and S depletions at the prior austenite grain boundaries. The relative absence of MnS precipitation in the specimens quenched 1 minute after reaching 1273 K (1000 °C) either means that MnS particles were too fine (<100 nm) to be resolved by EPMA or the Mn and S were still in solution. The low ductility indicates the former, which again, agrees with Goa and Sorimachi.[24]

The EPMA maps showed a network of S segregation within the matrix for the samples isothermally held. The influence of this network on hot ductility was not understood. Further study is required to clarify the formation and influence of this network.

E. *Role of Sulfur on Hot Ductility*

It has been established that S had a detrimental effect on ductility for the given experimental conditions (solution treatment and *in situ* melting), for steels C1 and C2. Since it is the amount of S that redissolves during solution treatment, which influences hot ductility, rather than the total S content, it is important to establish the amount of S that can be redissolved at 1623 K (1350 °C). Turkdogan[25] demonstrated that the solubility of S in austenite increases as the Mn addition decreases because of the effect of Mn on the activity coefficient of sulfur.

The solubility of MnS in austenite at a given temperature can be determined by solving the solubility product, k_s, of MnS (Eq. [1]), by using the solubility product of S (Eq. [2]), and its activity coefficient as a function of temperature (Eq. [3]).[1]

$$k_S = [\mathrm{Mn}][\mathrm{S}]f_S^{\mathrm{Mn}} \quad [1]$$

$$\log k_S = 2.929 - 9020/T \quad [2]$$

$$\log f_S^{\mathrm{Mn}} = [0.097 - 215/T][\mathrm{Mn}] \quad [3]$$

where [Mn] is the dissolved Mn content (wt pct), [S] is the dissolved S content (wt pct), $f_S^{Mn}$is the effect of Mn on the activity coefficient of S in austenite, and T is the temperature (Kelvin). Using the above equations, the solubility of S at 1623 K (1350 °C) for steel C1 was 0.012 pct and for steel C2, 0.008 pct. Owing to the low Mn content, the S solubility at 1623 K (1350 °C) was similar to the total S contents of steels C1 and C2 and therefore the behavior due to S would be expected to be similar for both test conditions, as the test results imply. The higher Mn level of steel C4 reduces the solubility of S at 1623 K (1350 °C) to only 0.0018 pct, which is similar to the total S level in the steel, but very little influence would be expected from such a low S content on hot ductility.

The embrittlement of low carbon steels with low Mn/S ratios due to the precipitation of MnS at the austenite grain boundaries during cooling to the test temperature is a known phenomenon.[9–11] Low carbon steels with similar Mn/S ratios (15 and 30) to steel C1 (19.1) were tested by Suzuki *et al.*,[10] and low ductility was observed between 1123 K and 1423 K (850 °C to 1150 °C), a similar range as observed for this study. Low ductility was attributed to precipitation of MnS at austenite grain boundaries. A significant increase in the carbon content and higher Mn/S ratio (52.5) of steel C3 appears to inhibit the precipitation of MnS at austenite grain boundaries as indicated by the excellent ductility observed above the Ae_3 temperature.

F. *Commercial Findings*

Steels C1 and C2 both showed very low ductility at and above 1273 K (1000 °C) for solution treatment and *in situ* melt conditions; this indicates a high likelihood for developing transverse cracks during continuous slab casting. As discussed previously, a combination of large grain size and segregation of S to the austenite grain boundaries resulted in this low ductility. Plant experience reveals that there is no issue with cracking in these grades.[26] Results indicate that the given test conditions promoted the segregation of Mn and S to austenite grain boundaries, where on cooling, the decreasing solubility of S induced fine precipitation of MnS at austenite grain boundaries, contributing to the very low ductility observed.

This discrepancy with commercial experience is explained because of the oversimplification of the thermal history of a continuously cast slab. From modeling data of the surface temperature of steel C1 during continuous casting, key points of the thermal history are outlined: the surface temperature drops rapidly after exiting the mold at approximately 500 K/min to 1293 K (1050 °C); the slab is then cooled slowly to the unbending segment, taking approximately 9 minutes and the temperature decreases to 1153 K (880 °C) and during this cooling period thermal oscillations take place, where rapid cooling [~273 K (~100 °C)] and reheating occurred in the roll bite.[26] The rapid cooling would limit segregation to the austenite grain boundaries and the slow cooling afterward would coarsen any MnS at prior austenite boundaries, diminishing their

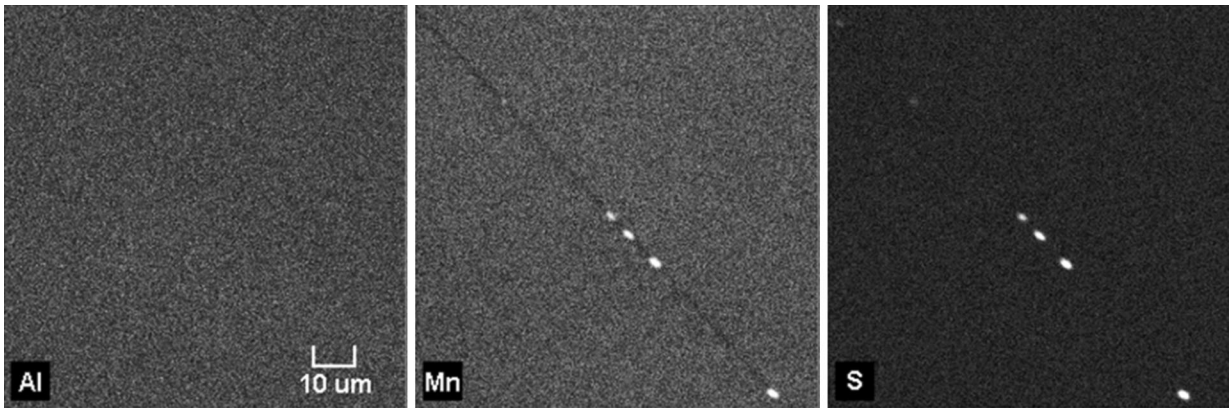

Fig. 7—EPMA image: C1 *in situ* Melt condition, held for 1 min at 1273 K (1000 °C), and then quenched.

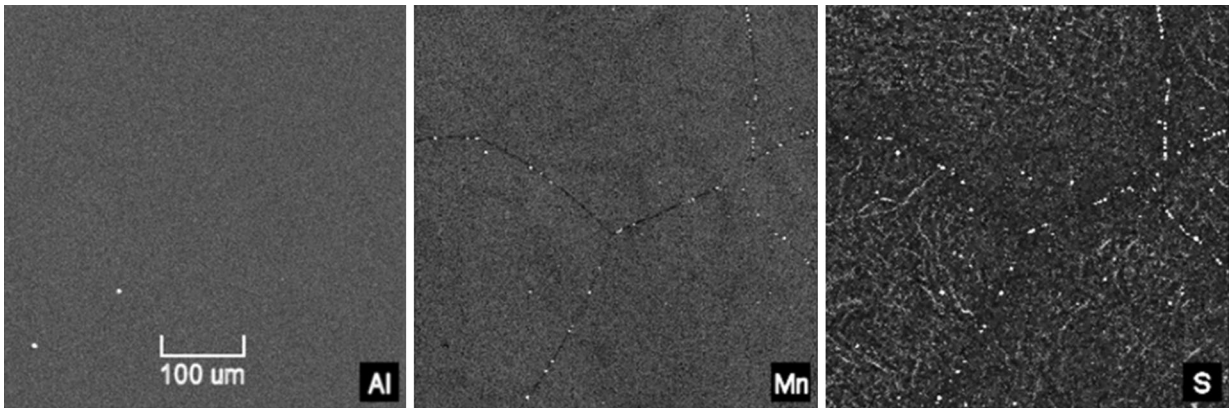

Fig. 8—EPMA image: C1 solution treatment at 1623 K (1350 °C), held for 10 min at 1273 K (1000 °C), and then quenched.

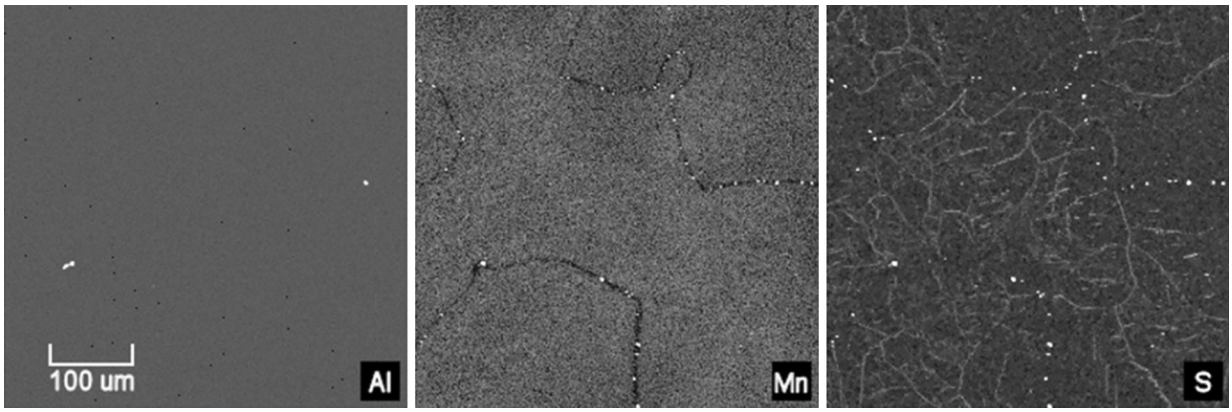

Fig. 9—EPMA image: C1 *in situ* Melt condition, held for 10 min at 1273 K (1000 °C), and then quenched.

influence on hot ductility. The isothermal holding tests showed a dramatic improvement in ductility because of the coarsening of the MnS at austenite boundaries. The longer hold time more appropriately reflects the longer time taken for a slab to cool to the unbending temperature in practice, which agrees well with the absence of ductility issues observed in commercial experience.

Second, the solidification, segregation pattern, and thermal histories in a large slab cannot be reproduced in a small tensile sample. In other words, the significant differences in scale will substantially increase time for solidification, leading to coarse, macro segregation. As a slab solidifies, enrichment of the liquid preceding the dendrite growth leads to increased segregation between dendrite arms. Owing to the very slow solidification rate in thick slabs compared with the rapid solidification in small tensile samples, the secondary dendrite arm spacing is much coarser in slabs and thus, the segregation pattern and microstructures formed are different.

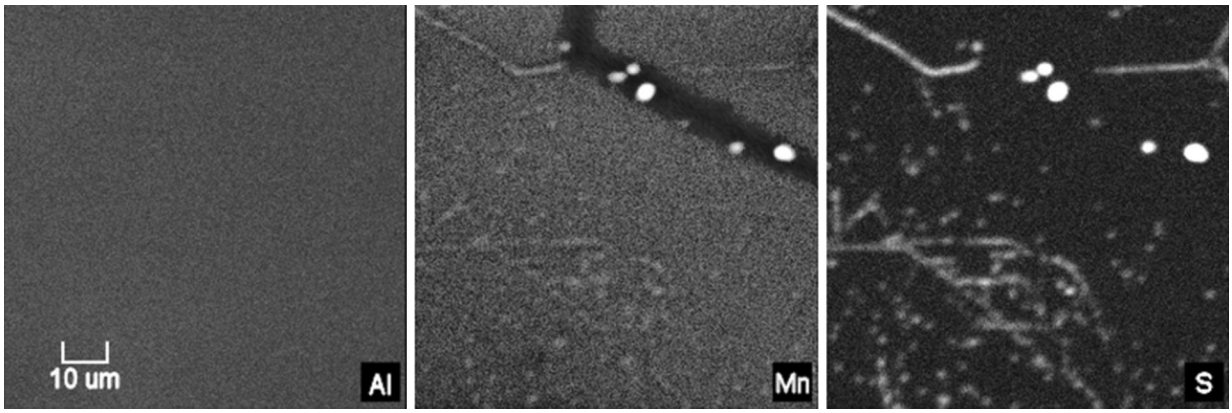

Fig. 10—EPMA image: Higher magnification of Fig. 9; C1 *in situ* Melt condition, held for 10 min at 1273 K (1000 °C), and then quenched.

A solidifying strand is also subject to ferrostatic pressure which, in conjunction with the strand alternating between caster rolls, causes fluid flow in the liquid that can "wash away" the tips of advancing dendrites, further enhancing segregation. It is known that MnS precipitates in segregated areas, such as between dendrite arms in continuously cast slabs, leading to significant precipitation within austenite grains and decreasing the availability of S to segregate to austenite grain boundaries, which would be beneficial for hot ductility. On the other hand, in small cylindrical specimens for hot ductility testing, the finer solidification pattern leads to reduced segregation, less precipitation of MnS, and therefore increased availability for S to segregate to austenite grain boundaries.

V. CONCLUSIONS

Hot ductility testing was performed on low carbon steels with a range of Mn/S ratios at a low strain rate of 7.5×10^{-4} s^{-1}. Solution treatment, *in situ* melting, and isothermal holding patterns were performed to establish the effect of thermal history and Mn/S ratio on hot ductility. The results obtained were as follows:

1. At less than the Ae_3 temperature, steels, C1, C2, and C3 showed ductility troughs for both solution treatment and *in situ* melting conditions because of transformation controlled intergranular failure along thin films of ferrite at prior austenite boundaries, where MnS precipitation within these films enhanced the failure mechanism.
2. At greater than the Ae_3 temperature, steel C3 showed excellent ductility, while the low C, low Mn steels, C1 and C2, exhibited a wide and deep ductility trough, because of intergranular grain boundary failure *via* grain boundary sliding, enhanced by precipitation of MnS at austenite grain boundaries.
3. Isothermal holding at 1273 K (1000 °C) for 10 minutes, before tensile testing, substantially improved hot ductility for the steel C1 because of coarsening of MnS at austenite grain boundaries as identified by EPMA.
4. Steel C4 showed good ductility at all test temperatures for solution treatment tests because of grain refinement caused by the Nb and Ti microalloying additions. For *in situ* melting conditions, this grain-refinement ability was lost and ductility was significantly lower because of the detrimental effects of large grain size combined with fine microalloyed precipitates.
5. The commercial production of steels C1 and C2 do not have any cracking issues during continuous casting, contrary to indications from hot ductility simulations. This discrepancy appears to be because of a marked difference in precipitation behavior because of the oversimplification of the thermal history for the hot ductility test program. A simplified hot ductility test was found to be inadequate for investigating the potential of low C, low Mn steels to develop transverse cracking, and it is recommended that future experiments are conducted using detailed simulations of the thermal history during continuous casting.

ACKNOWLEDGMENTS

The current study was conducted at the University of Wollongong under a funding support from BlueScope Steel, Australia. The authors wish to thank Mr. Les Moore for conducting the EPMA analysis and assisting with interpretation of the results.

REFERENCES

1. T. Gladman: *The Physical Metallurgical of Microalloyed Steels*, The Institute of Materials, London, 1997, p. 312.
2. A. Cowley and B. Mintz: *Mater. Sci. Technol.*, 2004, vol. 20, pp. 1431–39.
3. B. Mintz and Z. Mohamed: *Mater. Sci. Technol.*, 1989, vol. 5 (12), pp. 1212–19.
4. B. Mintz, S. Yue, and J.J. Jonas: *Int. Mater. Rev.*, 1991, vol. 36 (5), pp. 187–217.
5. B. Mintz and R. Abushosha: *Mater. Sci. Technol.*, 1992, vol. 8 (2), pp. 171–77.

6. R. Abushosha, S. Ayyad, and B. Mintz: *Mater. Sci. Technol.*, 1998, vol. 14 (3), pp. 227–35.
7. B. Mintz: *ISIJ Int.*, 1999, vol. 39 (3), pp. 833–55.
8. B. Mintz and J. R. Banerjee: *Mater. Sci. Technol* 2010, vol. 26 (5), pp. 547–551.
9. H. Kabayashi: *ISIJ Int.*, 1991, vol. 31 (3), pp. 268–77.
10. M. Suzuki, C.H. Yu, H. Shibata, and T. Emi: *ISIJ Int.*, 1997, vol. 37 (9), pp. 862–71.
11. K. Yasumoto, Y. Maehara, S. Ura, and Y. Ohmori: *Mater. Sci. Technol.*, 1985, vol. 1 (2), pp. 111–16.
12. B. Mintz, R. Abushosha, O.G. Comineli, and M.A. Loyola de Oliveira: *THERMEC'97: International Conference on Thermomechanical Processing of Steels & Other Materials*, Wollongong, 1997, pp. 867–73.
13. Y. Maehara, K. Yasumoto, H. Tomono, T. Nagamichi, and Y. Ohmori: *Mater. Sci. Technol.*, 1990, vol. 6 (9), pp. 793–806.
14. K.M. Banks, A. Tuling, and B. Mintz: *Mater. Sci. Technol.*, 2012, vol. 28 (5), pp. 536–42.
15. B. Mintz, J.M. Stewart, and D.N. Crowther: *Trans. Iron Steel Inst. Jpn.*, 1987, vol. 27, pp. 959–64.
16. A.M. El-wazri, F. Hassani, S. Yue, and E. Es-sadiqi: *Iron Steelmak*, 1998, vol. 1, pp. 37–41.
17. A.M. El-wazri, F. Hassani, S. Yue, E. Es-sadiqi, L.E. Collins, and K. Iqbal: *ISIJ Int.*, 1999, vol. 39 (3), pp. 253–62.
18. S. Akhlaghi, F. Hassani, and S. Yue: *40th MWSP Conf. Proc.*, pp. 699–705, Pittsburgh, PA, ISS., Oct 25–28, 1998.
19. K.W. Andrews: *J. Iron Steel Inst.*, 1965, vol. 203, pp. 721–29.
20. C. Chimani, G.X. Shan, K. Morwald, O. Kolendnik, H.J. Bohm, D. Duschlbauer, and T. Drabek: *AISTech 2006 Proceedings*, vol 1, pp. 825–830, AIST, Warrendale, PA, May 1–5, 2006.
21. Y. Maehara and T. Nagamichi: *Mater. Sci. Technol.*, 1991, vol. 7 (10), pp. 915–21.
22. K. Carpenter: Ph.D. Thesis, Faculty of Engineering, University of Wollongong, NSW, 1994.
23. A. Mannucci, E. Anelli, M. Armengol, and M. Vedani: *MSF*, 2010, vols. 638–642, pp. 3362–67.
24. Y. Gao and K. Sorimachi: *ISIJ Int.*, 1995, vol. 35 (7), pp. 914–19.
25. E.T. Turkdogan, S. Ignatowicz, and J. Pearson: *J. Iron Steel Inst.*, 1955, vol. 180, p. 349.
26. X. Tsekouras: Private Communication, BlueScope Steel, Five Islands Road, Port Kembla, NSW, 2010.